Supplementary material for

Middle Pleistocene fluid infiltration with 10-15 ka recurrence within the seismic cycle of the active Monte Morrone Fault System (central Apennines, Italy)

by Vignaroli et al.

This supplementary material consists of:

- Table A1
- Table A2
- Figure SM1
- Figure SM2
- Figure SM3

Table A1. Stable oxygen and carbon isotope composition of the selected samples from the Monte Morrone Fault System collected at the studied outcrop near Roccacasale village (long.: 13.883°; lat.: 42.125°). Isotope compositions are expressed in ‰ against Vienna Pee Dee Belemnite standard (VPDB).

Sample	Description	$\delta^{13}C$ (‰ VPDB)	$\delta^{18}O$ (‰ VPDB)
nM4G	Calcite mineralisation (top)	-9.67	-11.32
nM4G_1	Calcite mineralisation 1	-9.35	-11.36
M4G_1a	Calcite mineralisation 1	-9.41	-11.03
M4G_1b	Calcite mineralisation 1	-9.25	-11.39
M4G_1c	Calcite mineralisation 1	-9.10	-11.04
M4G_1d	Calcite mineralisation 1	-9.25	-11.65
M4G_1e	Calcite mineralisation 1	-9.24	-11.31
M4G_1N	Calcite mineralisation 1	-7.82	-7.69
nM4G_2	Calcite mineralisation 2	-7.66	-7.57
M4G_2a	Calcite mineralisation 2	-7.82	-8.09
M4G_2b	Calcite mineralisation 2	-7.98	-8.07
M4G_2c	Calcite mineralisation 2	-8.23	-8.23
M4G_2d	Calcite mineralisation 2	-8.26	-7.93
M4G_2e	Calcite mineralisation 2	-7.41	-7.58
M4G_2N	Calcite mineralisation 2	-8.23	-8.10
nM4G_3	Calcite mineralisation 3	-9.35	-8.17
M4G_3a	Calcite mineralisation 3	-9.51	-8.35
M4G_3b	Calcite mineralisation 3	-9.57	-8.54
M4G_3c	Calcite mineralisation 3	-9.33	-8.49
M4G_3d	Calcite mineralisation 3	-9.58	-8.59
M4G_3e	Calcite mineralisation 3	-9.47	-8.52
M4G_3N	Calcite mineralisation 3	-9.32	-8.24
M4G_4N	Matrix of breccias (protocataclasite)	-1.35	-3.33
M4G_5N	Cataclasite matrix	0.19	-1.83
nM4G_4	Cataclasite matrix	-1.13	-3.04
M4HW	Calcite mineralisation	-8.63	-8.49
nM4HW	Calcite mineralisation	-8.24	-8.62
nM4HW_c	Cataclasite matrix	0.54	-2.08
M4HW_a	Calcite mineralisation	-8.70	-8.80
M4HW_1N	Protolith in cataclasite matrix	2.27	-0.44
M4HW_2N	Protolith in cataclasite matrix	1.40	-1.28
M4HW_3N	Calcite mineralisation	-8.51	-8.62
M4HW_4N	Calcite mineralisation	-8.07	-10.42
M4H2_1	Calcite mineralisation	-8.92	-8.74
M4H2_2	Calcite mineralisation	-9.35	-8.42
M4H	Calcite mineralisation	-9.14	-9.89
nM4H	Calcite mineralisation	-9.07	-8.90
nM4H_c	Cataclasite matrix	-8.67	-9.04
M4H_P	Protolith in cataclasite matrix	2.38	-0.43
nM4i_1	Calcite mineralisation	-8.84	-8.87
nM4i_2	Calcite mineralisation	-10.46	-9.18
nM4i_3	Calcite mineralisation	-8.82	-9.21
M4i_1	Calcite mineralisation	-9.63	-8.78

M4i_2	Calcite mineralisation	-10.44	-9.29
nM4F1_1	Calcite mineralisation	-9.74	-7.99
nM4F1_2	Calcite mineralisation	-10.22	-7.85
M4F1_1	Calcite mineralisation	-10.01	-7.37
M4F1_2	Calcite mineralisation	-7.14	-8.21
nM4d_P	Protolith in cataclasite matrix	1.89	-1.32
nM4d_m	Cataclasite matrix	0.61	-2.00

Table A2. Clumped isotopes analyses on the selected samples from the Monte Morrone Fault System.

Sample number	Sample type	Replicate measurements	$\delta^{13}C$ (VPDB)	$\delta^{18}O$ (VPDB)	$\delta^{18}O$ (VSMOW)	Δ_{47} (I-CDES)	Std. Dev. (1σ)	T (°C)	Std. Dev. (1 σ)	SE	95% CL	$\delta^{18}O$ Fluid (VSMOW)
M4 F1 2	Carbonate mineralisation	12	-7.23	-8.32	22.35	0.552	0.032	40	10.8	3.1	6.9	-3.0
M4 G 1b	Carbonate mineralisation	9	-9.25	-11.35	19.22	0.594	0.025	24	7.6	2.5	5.8	-9.2
M4 G 1e	Carbonate mineralisation	9	-9.16	-11.27	19.30	0.598	0.013	23	3.7	1.2	2.9	-9.3
M4 G 2a	Carbonate mineralisation	9	-7.72	-8.04	22.63	0.591	0.025	26	7.5	2.5	5.8	-5.5
M4 G 2b	Carbonate mineralisation	11	-7.93	-8.07	22.60	0.600	0.019	23	5.8	1.8	3.9	-6.9
M4 G 3c	Carbonate mineralisation	12	-9.33	-8.47	22.19	0.590	0.044	26	14.1	4.1	9.0	-5.9
M4 G 5N	Cataclasite	9	-0.40	-1.77	29.09	0.548	0.026	41	9.0	3.0	6.9	3.7
M4 HW 1N	Clast in cataclasite	11	2.04	0.11	31.04	0.540	0.032	45	10.9	3.3	7.3	6.3

I-CDES: Intercarb Carbon dioxide equilibration scale (Bernasconi et al., 2021) with uncertainty in temperature reported at the 95% confidence level (CL).

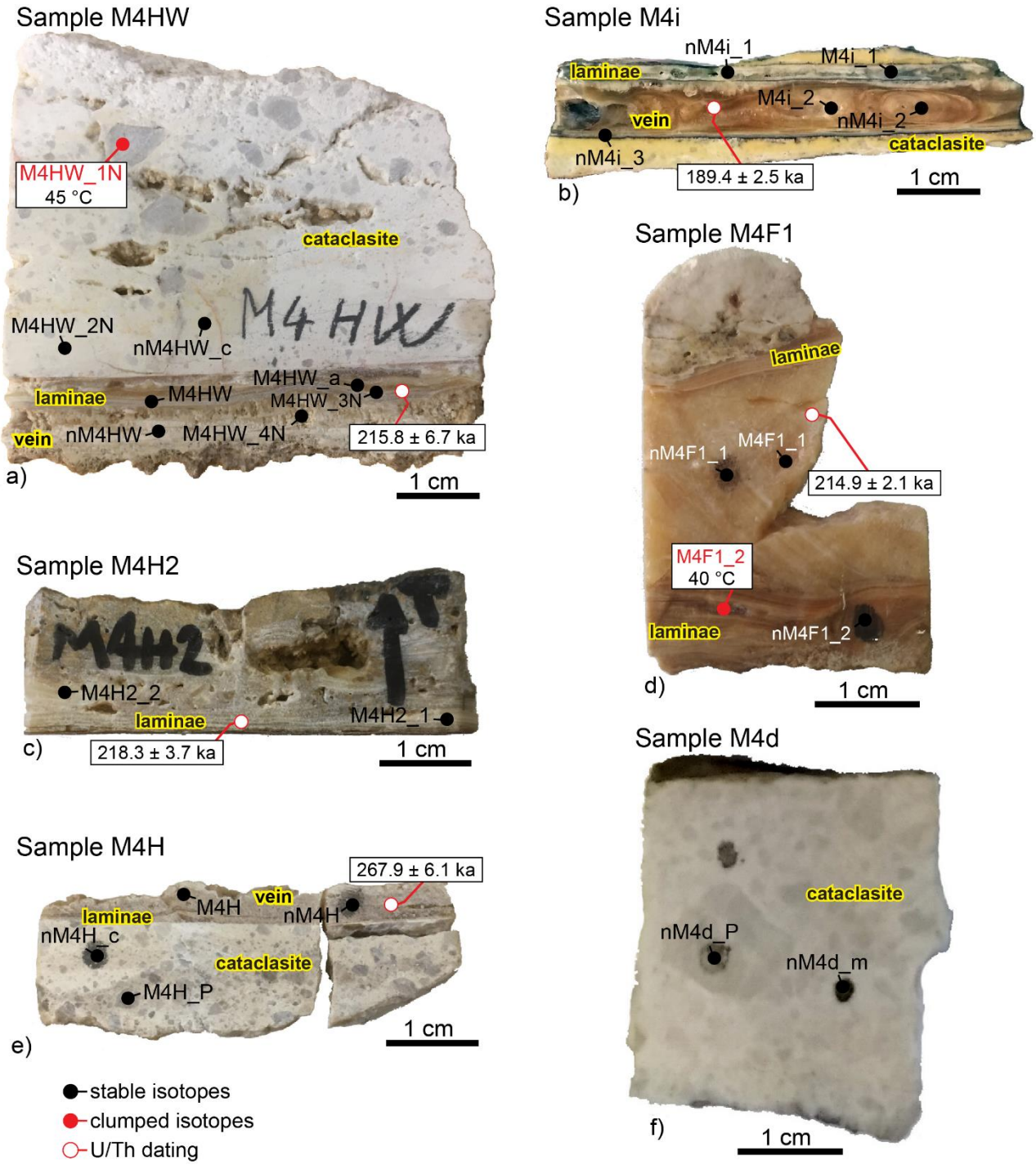

Figure SM1. Polished rock slabs of the analysed samples (sample M4G is reported in Fig. 5; Tables 1 and 2) with the indication of micro-drilling sites for geochemical (stable isotopes in black and clumped isotopes in red) and geochronological analysis (red-white circles). U-Th ages and temperatures deriving from clumped isotopes analysis are also indicated.

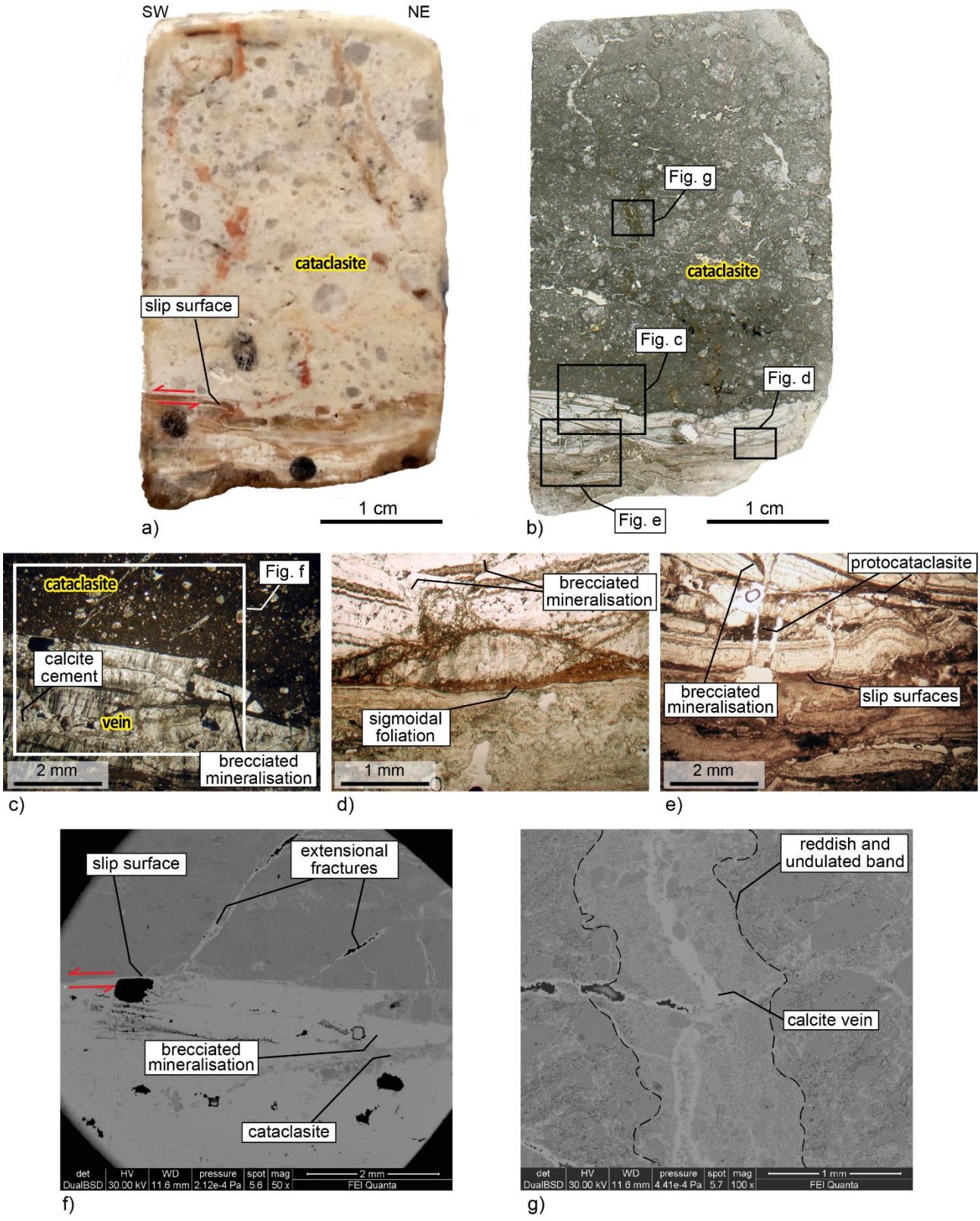

Figure SM2. Polished slab, high-resolution scanned thin section, detailed petrographic and back-scattered electron (BSE) images showing the main observed structural fabrics of sample M4HW. a) Oriented polished rock slab showing the contact between the slip surface (here developed at the top of the carbonate mineralisation) and the hanging wall of the massive cataclasite; b) high-resolution scanned thin section of sample M4HW showing the carbonate mineralisations (at the bottom) and cataclasite (at the top); c) petrographic image (crossed polarised light) showing brecciated mineralisations partially embedded within the fine-grained cataclasite. Secondary cement made by calcite crystals occurs within the reworked carbonate

mineralisations; d) petrographic image (plane polarized light) showing sigmoidal foliation within the carbonate mineralisations embedded in two minor slip surfaces; e) petrographic image (plane polarised light) showing fractured and brecciated carbonate mineralisations with several minor slip surfaces and embedding pockets of protocataclasites; f) BSE image showing the main slip surface at the top of the carbonate mineralisations and the fractured mineralisations partially embedded in the cataclasite. Note the two extensional fractures developed along the main slip surface; g) BSE image showing structures high angle to vertical slip surface, generally with undulating boundaries and characterised by tight cataclasite and calcite vein.

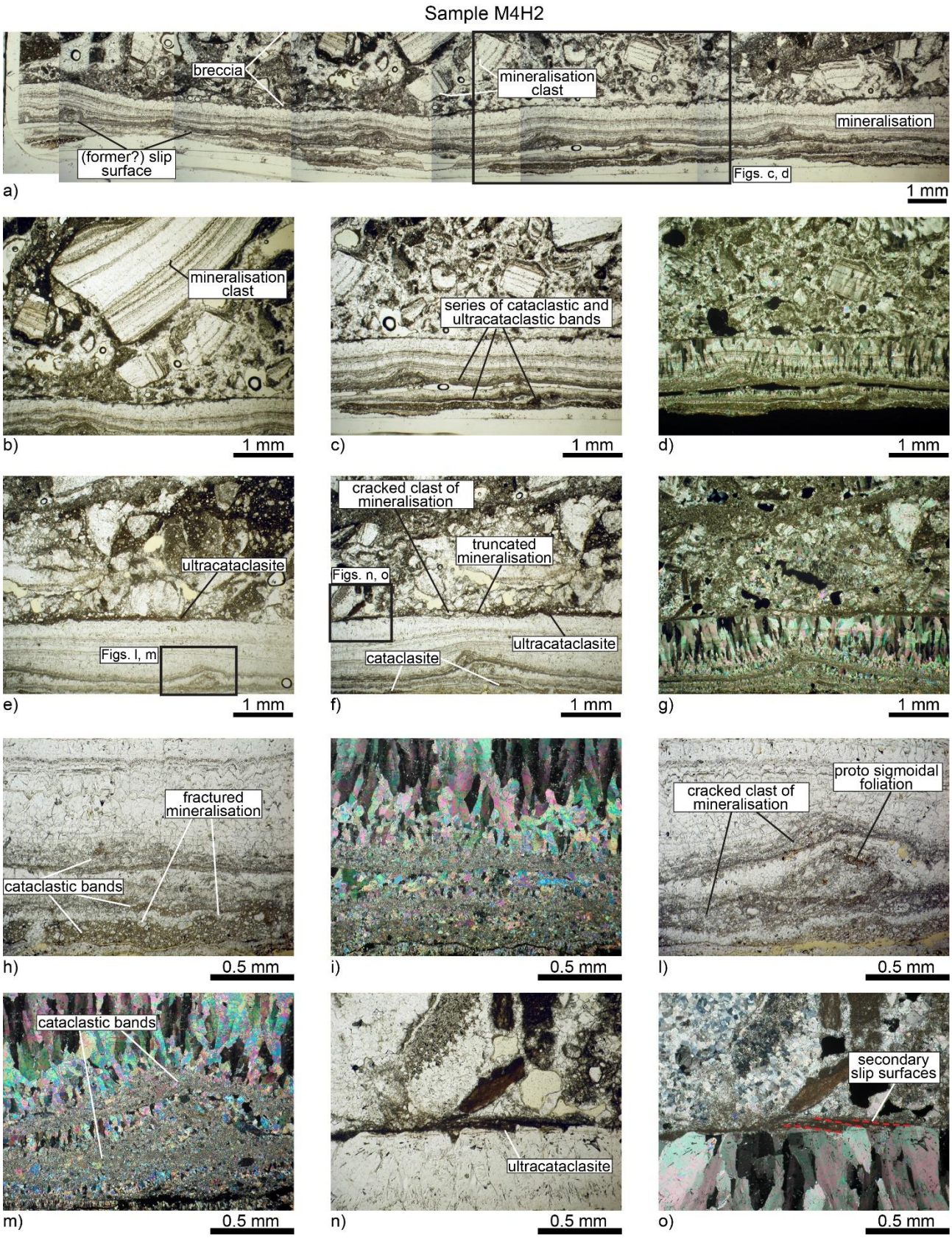

Figure SM3. Petrographic images showing the microscale properties of M4H2 sample at different scale of observation. (a) Petrographic photomosaic (plane polarised light) of the lower part of M4H2 thin section showing (at the bottom) multiple generation of mineralisations (formed both by laminae and veins) and breccia (at the top). The upper edge of the mineralisation is characterized by a thin layer of ultracataclasite. At least one slip surface is observed within the mineralisation. (b) Petrographic image (plane polarised light)

showing within the breccia clasts of former mineralisations mixed with other carbonate fragments deriving from previous cataclasite and calcite cement. (c-d) Petrographic images (plane and crossed polarised light, respectively) showing a series of bands of cataclasite and ultracataclasite within the mineralisation. (e) Petrographic image (plane polarised light) showing the upper edge of the mineralisation covered by a thin layer of ultracataclasite. (f-g) Petrographic images (plane and crossed polarised light, respectively) showing a series of bands parallel to the slip surface and formed by cataclasites alternating with highly fractured mineralisations. The upper portion of the mineralisation is flattened and truncated along the slip surface and some fragments of the mineralisation are partially embedded within the thin layer of ultracataclasite. (h-i) Petrographic images (plane and crossed polarised light, respectively) showing in detail a series of bands parallel to the slip surface and formed by cataclasites alternating with highly fractured mineralisations. Interposed between two bands of cataclasite, a thin level of mineralisation is highly fractured, and some carbonate clasts are partially dispersed in the cataclasite. (l-m) Petrographic images (plane and crossed polarised light, respectively) showing a highly fractured portion of the mineralisation with a shape miming a sigmoidal foliation. (n-o) Petrographic images (plane and crossed polarised light, respectively) showing in detail the upper portion of the mineralisation. A thin layer of ultracataclasite, with some synthetic shear zone, covers the edge of the mineralisation.